Moisture Studies of a Self-Drying Roof: Tests in the Large-Scale Climate Simulator and Results from Thermal and Hygric Models

André O. Desjarlais **Thomas W. Petrie, Ph.D.** *Member ASHRAE* **Phillip W. Childs** **Jerald A. Atchley**

ABSTRACT

Simultaneous experiments on the moisture behavior of six low-slope roof systems were performed in a climate simulator. The systems were composed of a self-drying design over a conventional metal deck, a self-drying design over a significantly more permeable slotted metal deck, and four other systems over conventional metal decks: a system typical of U.S. construction with a liquid water permeable vapor retarder, a system typical of European construction with a liquid water permeable vapor retarder, a top-ventilated system with a polyethylene vapor retarder, and an impermeable control system with a polyethylene vapor retarder. The total weight of each test panel was measured and recorded continuously, along with temperatures and heat fluxes, to compare the behavior of the various systems. We imposed steady-state temperatures from hot summer to cold winter conditions to obtain the R-values of the construction dry insulations in each panel. Temperature cycles typical of hot summer days and mild winter days were then imposed above the construction dry assemblies to obtain baseline diurnal performance.

Enough water was added under the membrane of each system to saturate a layer of blotting paper. During the repeated diurnal cycles typical of hot summer days, the self-drying design over the slotted deck dried fastest, followed by the European construction with a liquid water permeable vapor retarder, then the self-drying design over the solid deck. When water was added to the systems, the lower membrane of the top-ventilated system had been slit in several places and this system dried at a slow rate. When the lower membrane was removed completely, the top-ventilated system dried as fast as the self-drying design over the solid deck. The control system and the U.S. construction with a liquid water permeable vapor retarder dried slowly at about the same rate. We applied a one-dimensional thermal and hygric model. The solid and slotted deck were assumed to differ only in water vapor permeance. A model was not attempted for the top-ventilated system. The 1-D model predicted very well the slow rates of wetting in the winter cycles and both the slow then fast rates of drying in the summer cycles before and after water addition; however, it overpredicted the drying rate for the U.S. construction with a liquid water permeable vapor retarder.

INTRODUCTION

An ongoing U.S. DOE-sponsored program of research at a national laboratory focuses on issues concerning drying of low-slope roof systems. Experience with low-slope roofs indicates that eventually they get wet from leaks through the membrane, especially around penetrations and flashings. This experience begs the questions: Will some wetted roofs dry out by themselves? How quickly? What combination of components allows them to dry faster?

Moisture in low-slope roof systems degrades the thermal value of the insulation and corrodes metal decks and fasteners. Rapid drying rates allow wet materials to dry before damage occurs. If a roof system has an inherently fast drying rate, elimination of a leak by repair of the damaged area or re-cover over the existing system is all that is required. Removal and disposal of wet materials, which are especially costly if asbestos materials are involved, would not be needed.

Detailed results (Pedersen et al. 1992) and a summary (Desjarlais et al. 1993) of the initial work in this program of research documents the effects of moisture movement on the thermal efficiency of low-slope systems insulated with fibrous glass. A solid polyethylene vapor retarder, polyethylene with small holes, a liquid water permeable vapor retarder, and no vapor retarder over the gypsum board decks were the differences among the systems in this series of experiments. Electrical capacitance moisture probes (Motakef and Glicksman 1989) and plywood electrical resistance probes were used to

Andre O. Desjarlais is program manager, **Thomas W. Petrie** is a research engineer, and **Phillip W. Childs** is a staff engineer at the Buildings Technology Center, Oak Ridge National Laboratory, Oak Ridge, Tenn. **Jerald A. Atchley** is a technician at Lockheed Martin Energy Research, Oak Ridge, Tenn.

follow moisture movement. Because of uncompensated temperature effects with the capacitance probes, the resistance probes were more successful in reporting changes in moisture levels within the panels. However, they were very slow to respond. Components of the systems were removed periodically and weighed to provide a measure of overall weight loss from the panels.

Unique indicators of moisture movement turned out to be the pair of small, thermopile-type heat flux transducers embedded in the top and bottom of each panel's insulation. These transducers are designed to indicate sensible heat flux as a result of the small temperature difference that occurs across them when they are buried in hygroscopic or water vapor permeable materials through which heat is flowing. In general, we calibrate heat flux transducers in the same materials in which they are to be used. When, in these early tests, we placed them in direct contact with a water impermeable surface, such as the vapor retarders at the bottom of some panels, if water condensed on them, it augmented the apparent heat flux. They indicated more than the sensible heat flux. In further work, we have avoided this complication and placed heat flux transducers in locations where condensation does not occur on them.

When roof systems, such as one with a solid polyethylene vapor retarder over the deck and a single-ply impermeable membrane over the insulation, have moisture trapped in them, the moisture can significantly increase the heat flux. For diurnally varying membrane temperatures typical of summer conditions, latent and sensible heat fluxes are possible if nighttime conditions allow condensation of moisture on the vapor retarder. A one-dimensional heat and mass transfer numerical model (Pedersen 1990) successfully predicted the total heat flux when only sensible or both sensible and latent heat fluxes were contributing.

A second series of tests was undertaken with various insulation materials over plywood decks covered by impermeable single-ply membranes and, later in the series, by additional re-cover insulation (Desjarlais et al. 1994). Fiberboard, perlite, fibrous glass, and polyisocyanurate were the insulation materials used under the membranes. After tests with construction dry materials to ascertain their thermal properties and fine tune the climate control systems above and below the test sections, water was deliberately added to all test sections. Diurnally varying temperatures typical of a sunny summer day in Knoxville, Tennessee, were imposed. Re-cover insulation was added without an additional membrane, and the summer cycles continued. Then, conditions typical of a sunny winter day in Knoxville were imposed with and without the re-cover insulation. In these experiments, heat fluxes were measured in the middle of the permeable insulations, yielding sensible heat fluxes through the middle of the assemblies.

The unique measurement in this second series of tests was continuous monitoring of the total weight of each panel, made possible by suspending each panel from load cells. The record of weight changes showed that the climate significantly affected drying rates for all configurations. The Knoxville summer condition accelerated the rate of drying, and the winter condition still allowed drying although at a much reduced rate. Re-cover caused slightly reduced rates of drying in summer but increased the drying rate in winter. The detailed record of weight change also allowed a combined heat and mass transfer model to be validated for these combinations of deck material and insulations. From the measurements and modeling, the permeance of the deck was identified as a key parameter in controlling drying rate in summer. In winter, if the deck is much less permeable to water vapor than the insulation, it again dominates drying rate. Otherwise, the insulation's permeance controls.

In the early 1970s, Powell and Robinson (1971) suggested that a roof design with in-service self-drying characteristics is the most practical and economic solution to extending the service life of roofs. The *NRCA Roofing and Waterproofing Manual* (NRCA 1996) defines a self-drying roof: "In concept, to qualify as a self-drying roof, the roof assembly must dissipate enough moisture during the drying season to reestablish an acceptable equilibrium moisture content for the materials used, so that at the end of each drying season the materials are not degraded and the thermal resistance of the insulation is not impaired. Also, there obviously must not be a trend toward long-term accumulation of moisture within the building or roof assembly."

Motivated by the soundness of Powell and Robinson's suggestion, Kyle and Desjarlais (1994) proposed methods to construct new roofs and retrofit existing roofs to make them self drying. They estimated the implications for the U.S. economy if there was significant penetration of the roofing market by self-drying roofs. They described design mechanisms for constructing self-drying roof systems. From the exterior side downward, an updated general description of their self-drying roof is as follows: a membrane, insulation relatively permeable to water vapor, a crack-free wicking layer to disperse any liquid that leaks through cracks in joints of the first insulation layer, insulation relatively impermeable to water vapor, insulation relatively permeable to water vapor, and a vapor permeable deck. If a water-impermeable vapor retarder is required to prevent upward diffusion of interior moisture into the roof, a self-drying design is not possible. A liquid water permeable vapor retarder, which allows liquid water to flow downward but retards either upward or downward flow of water vapor, could allow a roof to meet the National Roofing Contractors Association (NRCA) definition.

This paper presents the results of experiments that use steady-state and diurnally cycling climatic conditions to determine the effect of low-slope roof construction features on drying rates before and after water addition. The roofs include two with the Kyle and Desjarlais self-drying design as well as typical U.S. and European constructions for low-slope roofs with liquid water permeable vapor retarders. These four roofs have water-impermeable single-ply membranes covering them. Two other roofs with solid polyethylene vapor retarders

are included in the experiments. One has a system for top-ventilation over it, while the other, covered by an impermeable single-ply membrane, serves as a control roof. All the roofs, except the top-ventilated system, are analyzed with a one-dimensional thermal and hygric model for wetting and drying rates during diurnally varying temperatures.

DESCRIPTION OF THE TEST PANELS AND THE EXPERIMENT

The experiments were performed in a large-scale climate simulator (LSCS) at a U.S. national laboratory. The features of the LSCS of special interest for these experiments have been described previously (Pedersen et al. 1992). Here, six instrumented test panels were tested simultaneously. A special diagnostic platform was used to contain all six panels and allow them to be lifted into the LSCS by a crane. Figure 1, a photograph taken during assembly of the test sections outside the LSCS, shows how an I-beam bisected the 13 ft (4 m) square inside area of the platform. The I-beam allowed two metal plates to be anchored above a side of each of the six test panels. A third metal plate for each panel was attached to the diagnostic platform itself to form a triangle with the other two plates for the panel. These plates supported the six test panels on three load cells apiece.

The specific configuration of each panel, including location of the thermocouples and heat flux transducer in each, is shown in Figure 2. Identification of the symbols and patterns used to depict the materials for construction and instrumentation of the panels is shown in Figure 3 (not to scale). The sizes of the thermocouple junctions between 26 gauge (0.40 mm) copper and constantan wires and the 2 in. (5.1 cm) square by 0.1 in. (2.5 mm) thick heat flux transducers have been exaggerated for illustrative purposes. The metal decks are shown with the same number of flutes as present in the 4 ft (1.2 m) wide assemblies. The flutes of both the solid metal deck and the slotted metal deck were open to the environmental chamber below the test sections. Air was circulated by fans around the perimeter of the chamber, where the dehumidification and humidification coils were located. The slotted metal deck was more permeable to air because there were four more flutes and because of two rows of 0.75 in. (19 mm) long by 0.050 in. (1.3 mm) wide slots, with 0.25 in. (6.4 mm) between each slot, running the entire 6 ft (1.8 m) lengths between each pair of flutes.

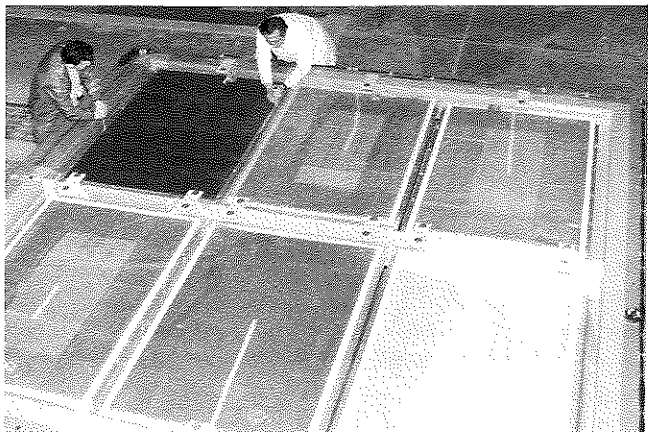

Figure 1 *Photograph of moisture panels during assembly showing the I-beam added to the center of the diagnostic platform and the metal plates for suspending the panels on load cells.*

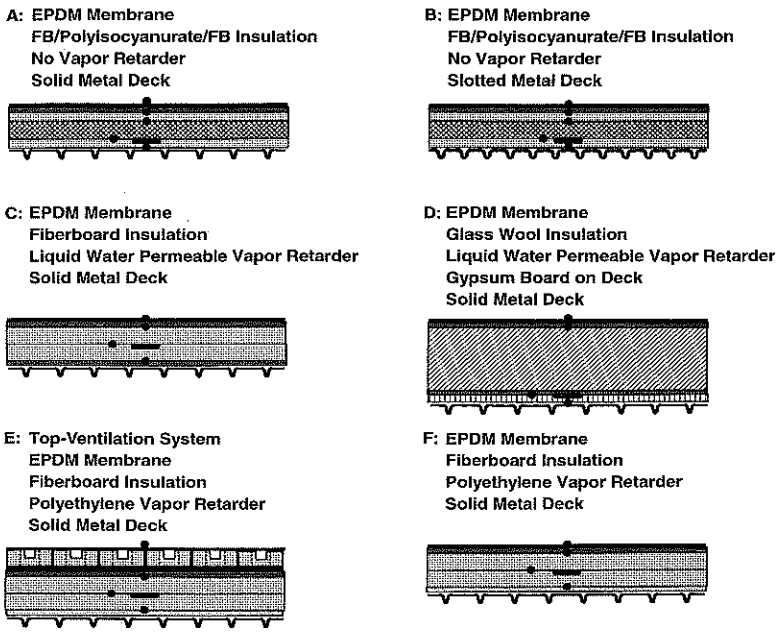

Figure 2 *Schematic details (not to scale) of the six panels, including locations of the thermocouples and heat flux transducer in each panel.*

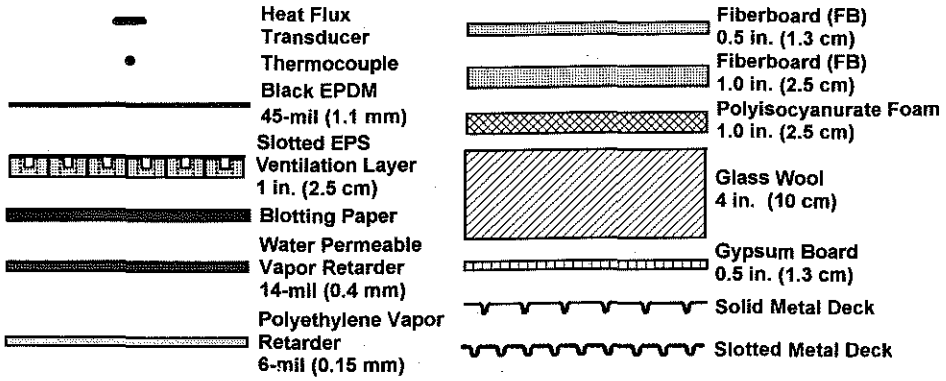

Figure 3 *Materials for construction and instrumentation of the panels and identification of the symbols and patterns used to depict them in Figure 2.*

Table 1 summarizes the material configurations for each assembly, R-values at 75°F (24°C) for the insulation in the construction dry assemblies, and the amount of water added before the last tests in this series. The R-values were determined in the initial tests. To further document how much water was added, it is also presented as a percentage by volume and weight of the insulation in each panel. The total thickness of the insulation for each configuration in Table 1 is 2 in. (5.1 cm) except for the European construction (Panel D), which had 4 in. (10.2 cm) of glass wool insulation (see Figures 2 and 3). Each system has an ethylene propylene diene monomer (EPDM) membrane and a layer of blotting paper under the EPDM to facilitate lateral movement of liquid water when it was added to

TABLE 1
Configuration, Insulation R-Value, and Water Addition for the Various Panels

Panel	Configuration	Insulation R-Value at 75°F (24°C) [h·ft²·°F/Btu (m²·K/W)]	Water Added [lb (kg)]	Water Added [% Insl. Volume (Weight)]
A	EPDM membrane FB/Polyisocyanurate/FB insulation No vapor retarder Solid metal deck	7.7 (1.4)	6.5 (2.9)	3.2 (22)
B	EPDM membrane FB/Polyisocyanurate/FB insulation No vapor retarder Slotted metal deck	7.7 (1.4)	8.0 (3.6)	3.9 (26)
C	EPDM membrane Fiberboard insulation Liquid water permeable vapor retarder Solid metal deck	5.1 (0.9)	8.3 (3.8)	4.0 (15)
D	EPDM membrane Glass wool insulation Liquid water permeable vapor retarder Gypsum board over solid metal deck	14.4 (2.5)	9.8 (4.4)	2.4 (20)
E	Slotted EPS top ventilation system EPDM membrane Fiberboard insulation Polyethylene vapor retarder Solid metal deck	5.1 (0.9)	6.9 (3.1)	3.4 (13)
F	EPDM membrane Fiberboard insulation Polyethylene vapor retarder Solid metal deck	5.1 (0.9)	8.6 (3.9)	4.2 (16)

the panels. The top-ventilated system also had a 1 in. (2.5 cm) thick piece of expanded polystyrene (EPS) and another EPDM membrane covering it. To produce the top-ventilated system, the supplier had cut 1 in. (2.5 cm) wide slots through the upper half of the EPS. The slots were equally spaced in both directions so as to leave squares of undisturbed EPS, with 3.75 in. (9.5 cm) long sides, in the upper half. The squares were originally connected by the solid lower half. To allow ventilation, circles 2.5 in. (6.4 cm) in diameter were bored through from top to bottom of the EPS at the intersection of the slots (see Figure 3 for a side view). The holes allow moisture to flow upward from the roof into the slots where crossflow of ventilation air through the slots can carry it out of the system.

Significant effort was made to eliminate leaks and to create one-dimensional heat and mass flow in the test panels. Figure 4 depicts the details of construction around the edge of each panel. To fabricate each test panel, an approximately 4 ft by 6 ft (1.2 m by 1.8 m) frame was constructed from 2 in. by 1¼ in. (51 mm by 32 mm) aluminum channel. The metal deck was bolted to the underside of the frame and sealed to it with a rubber gasket and silicone caulk. The flat space between flutes was sufficiently wide for mounting the retainers for the load cells. A 1 in. (2.5 cm) wide layer of 2 in. (5.1 cm) thick extruded polystyrene (XPS) was added inside the aluminum channel to thermally isolate the test specimen from the metal frame. The pieces of insulation in the test specimens were 42.5 in. wide by 67 in. long (1.08 m wide by 1.70 m long) and had no joints to form cracks through which water could leak. In a previous study (Desjarlais et al. 1994), a finite difference heat conduction code was used to verify that the thickness of the perimeter XPS insulation was sufficient to dampen out the effect of the thermal bridge due to the metal frame. For the amount of XPS used, the temperature at the edge of the panel insulation was calculated to be within 2°F (1°C) of the temperature at the center of the test panel.

Wide strips of 6 mil (0.15 mm) thick polyethylene were installed on all four edges between the aluminum channel and metal deck before the deck was bolted to the channel. The strips were wrapped over the interior surface of the XPS, with excess folded in the corners, and passed over the top surface of the aluminum channel. The purpose of the polyethylene was to reduce water vapor pickup in the XPS. The layer of blotting paper and the EPDM membrane were laid over the XPS and, along with the polyethylene strips, were held in place with 1/8 in. by 1 in. (3 mm by 25 mm) galvanized steel angle stock bolted into the frame along all four edges. An extra large piece of EPDM was cut for the second membrane on the top-ventilated system and for the European water permeable vapor retarder system so the EPDM could reach down to the steel bars. The two long edges were fastened for the top-ventilated system, leaving the two short edges exposed to conditions in the upper chamber. All four sides of the membrane over the European system were held down by the steel bars.

The excess polyethylene around each panel, shown draped over the I-beam and the Z-frame in Figure 4, was taped to the diagnostic platform or to the excess polyethylene from neighboring panels. This formed a crude seal between the upper and lower chambers but was by no means effective in preventing air and heat leaks between the two chambers. Better sealing was not attempted in order to not interfere with the measurement of the total weight of the panels by the trio of load cells from which each panel was suspended. The heating and cooling capacity in both chambers, as well as the dehumidification and humidification capacity in the lower chamber, were sufficient to hold desired conditions despite the air and heat leaks through the gaps between the panels and diagnostic platform and the very strong thermal bridges through the aluminum frame around each panel.

Figure 2 shows the placement of the four or five thermocouples and heat flux transducer for each panel. The Type-T (copper-constantan) thermocouples were installed at each interface inside the test panels (on top of the deck on a flat area between flutes, between the layers of insulation, and on top of the insulation) as well as on top of the membrane. In each panel, the 2 in. (5.1 cm) square thermopile-type heat flux

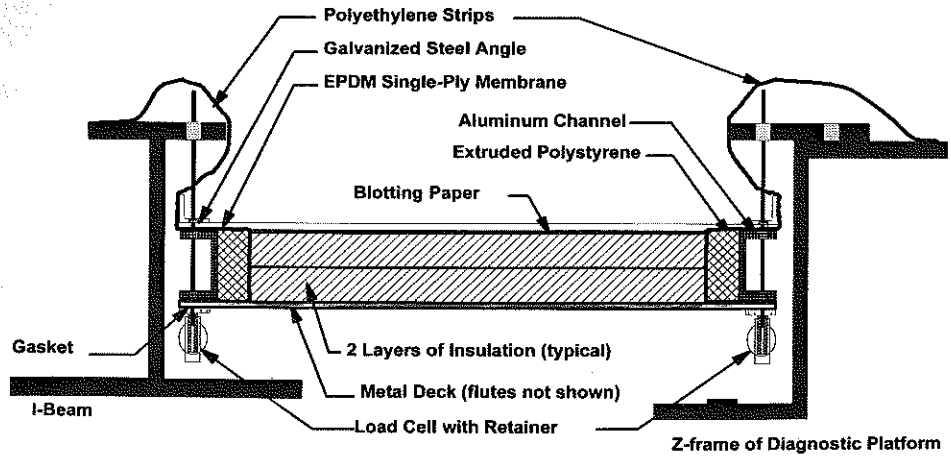

Figure 4 *Details of construction around the edge of each panel.*

transducer (HFT) was mounted in a small cutout between two insulation layers in the middle or toward the bottom of the assembly. Prior to their installation, the HFTs were calibrated in mock-ups of the test panels using instrumentation designed in accordance with ASTM C 518 (ASTM 1992).

Figure 4 shows one of the two load cells near the corners of the panels at one end and the third load cell in the center of the other end. The three strain gauge-type load cells were mounted to the underside of each metal frame. The cantilever of the load cell was attached to a thin metal rod that passed through a hole in the metal frame and was connected to the metal plates attached to the I-beam down the center of the diagnostic platform or to the diagnostic platform itself. This load cell configuration was used so that the load cells would be located in the lower chamber on the "building interior" side of the test panels. During the diurnal cycle experiments, this lower chamber was maintained at a constant temperature of approximately 70°F (21°C). Due to the thermal bridging and air leaks between chambers, the load cells were subjected to ±30°F (±17°C) variations about this temperature. The calibration of the load cells was done individually in a fixture that applied a dead load equal to about a third of the panel weight and then incremental loads to determine the cell's response for a small change in weight. Accurate reporting of panel total weight change by each trio was verified in-situ by placing calibration weights on each test panel after it had been suspended from its load cells.

Eight different experiments were performed, and conditions for each are listed in Table 2. Runs 1 through 3 were steady-state tests of the roof systems as a function of fixed thermal boundary conditions. The purpose of these experiments was to obtain baseline thermal performance data on the insulation materials in the roofing systems over the temperature range to which they would be subjected during the dynamic tests. A summary of the results for total insulation R-values is given in Table 1. These experiments also allowed us to verify that all the instrumentation was operating properly.

The remaining five runs were dynamic tests. During these tests, the lower chamber was controlled at 70°F (21°C) while the upper chamber air temperature was varied in diurnal cycles that represented clear sunny summer days (runs 4, 7, and 8) or clear sunny winter days (run 5) for a southern U.S. continental location (Knoxville, Tennessee). We included a run for colder but clear sunny winter days (run 6) in which we decreased the maximum and minimum temperatures relative to the Knoxville winter day. Only run 8 was done after the addition of water to the test panels.

The simulated climate temperatures in the upper chamber were selected such that the resulting roof surface temperatures were what we observed in outdoor tests in the actual Knoxville climate. We measured the membrane temperature cycles for several months in field tests on roofing systems with black membranes and averaged the data hour by hour. By trial and error, we adjusted the climate chamber air temperatures to achieve the membrane temperatures within 0.5°F (0.3°C) on average in each cycle. Figure 5 shows the upper-chamber air temperatures of the imposed cycles. For the Knoxville

TABLE 2
Summary of Experimental Conditions Imposed on Test Panels

Run	Moisture Content	Interior Conditions[a]	Exterior Conditions[a]
1	Hygroscopic	Fixed, 70°F (21°C), 47% RH	Fixed, 110°F (43°C), <10% RH
2	Hygroscopic	Fixed, 50°F (10°C), >90%RH	Fixed, 100°F (38°C), 17% RH
3	Hygroscopic	Fixed, 50°F (10°C), >90%RH	Fixed, 0°F (−18°C), 79% RH
4	Hygroscopic	Fixed, 70°F (21°C), 43% RH	Knoxville Summer Diurnal
5	Hygroscopic	Fixed, 70°F (21°C), 50% RH	Knoxville Winter Diurnal
6	Hygroscopic	Fixed, 70°F (21°C), 54% RH	Alternate Winter Diurnal
7	Hygroscopic	Fixed, 70°F (21°C), 50% RH	Knoxville Summer Diurnal
8	Water Added	Fixed, 70°F (21°C), 50% RH	Knoxville Summer Diurnal

[a] Interior conditions held in lower chamber; exterior conditions held in upper chamber.

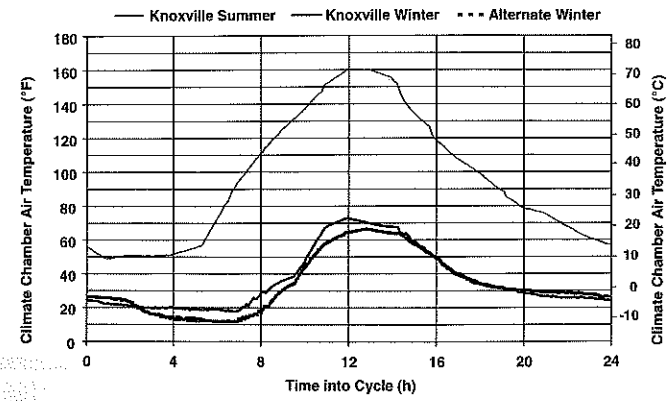

Figure 5 *Air temperatures in the climate chamber for the three different diurnal cycles imposed on the test panels.*

summer diurnal cycle, the upper chamber air temperatures were varied between 48°F and 160°F (9°C and 71°C); for the Knoxville winter diurnal cycle, they were varied from 18°F to 73°F (–8°C to 23°C); for the alternate winter diurnal cycle, they were varied from 11°F to 67°F (–12°C to 19°C). The relative humidity in the lower chamber was controlled, and in the final two tests, the target of 50% RH was achieved. The relative humidity in the upper chamber was not controlled but was monitored.

In runs 1 through 7, the water content of the test panels was due to the hygroscopic moisture content of the construction materials and, after run 1, any small amount of moisture lost or gained from previous runs. The heat flux transducers used to measure heat flow through each panel in the steady-state tests for the R-values in Table 1 were placed near the middle of the panels in relatively vapor permeable insulations. Their response was assumed not to be directly affected by moisture in the panels. Prior to constructing the panels, the materials used to fabricate the test panels were held at laboratory conditions of approximately 70°F (21°C) and uncontrolled ambient relative humidity (but generally 40% to 50%) for at least sixty days.

Between runs 7 and 8, the upper chamber was brought to room temperature and all the panels were blocked up so they were no longer suspended from the load cells. The angle bars holding down the membranes were removed on three sides. For the top-ventilated system, the top membrane and foam were removed to expose the lower membrane. The membranes were rolled back on all panels. Water was added by pouring water on the blotting paper and spreading puddles by hand to achieve reasonably uniform wetting. Several slits were cut in the lower membrane of the top-ventilated system to compromise its integrity. The other membranes were reattached to seal the water in each test panel. Table 1 shows the difference in panel weights due to water addition and percentages by volume and weight of insulation in each panel. Despite the variation from panel to panel due to some spillage, water addition was more than 2% by volume and 10% by weight of insulation in all panels.

Run 8 commenced with the test panels again exposed to the Knoxville summer diurnal cycle for seven cycles. It was obvious that the compromised membrane under the top-ventilated system was not allowing moisture to escape. The experiment was halted briefly to remove this membrane. The top-ventilated system, under this altered configuration, and the rest of the panels, with sealed membranes, continued through another six cycles to the end of the experiment.

EXPERIMENTAL RESULTS

Steady-State Dry Runs

The fixed temperature conditions listed in Table 2 for runs 1, 2, and 3 were held until eight hours of steady-state thermal performance data were obtained. Thermal resistivities (R-values per unit thickness) were calculated at each five-minute interval at which data were written to the data analysis spreadsheet for each run. These data were already the averages from the results of ten scans of the database at 30-second intervals, which were recorded in the historical data file for each run. Thermal resistivity is

$$r = \frac{\Delta T}{q \cdot t} \tag{1}$$

where

r = thermal resistivity, h·ft^2·°F/(Btu·in.) or m·K/W;

ΔT = temperature difference measured across the particular pieces of insulation in each panel (see Figure 2), °F or °C;

q = heat flux measured by the heat flux transducer in each panel, Btu/h·ft^2 or W/m^2;

t = thickness of the particular piece of insulation, in. or m.

In the first and second halves of the eight hours of steady state for each run, the maximum percent difference between average resistivities for each material was 0.6%. Although the climate simulator was not operated in guarded hot box mode in these tests, this is less than the maximum 1% variation allowed by ASTM C 236 for measuring steady-state thermal performance with guarded hot boxes (ASTM 1989).

Figure 6 shows the thermal resistivities vs. mean insulation temperature obtained from the three steady-state tests for the three insulation materials in the test panels. There were only two pieces of polyisocyanurate and one piece of glass wool in the six panels yielding six and three resistivities, respectively. There were ten pieces of fiberboard. Whether a piece was in the upper or lower part of a test panel affected the mean temperature it experienced during a test. Thus, a test panel with two pieces of fiberboard yielded six resistivities. There are 30 measurements shown for fiberboard in Figure 6. The scatter is likely due to variations in moisture content of the various pieces of construction dry fiberboard caused by the different locations and the slight movement of moisture in the steady-state tests. The fiberboard had a dry density of 16.5 lb/ft^3 (264 kg/m^3).

The best fit straight lines through each set of data are also shown in Figure 6. Later tests with pieces of polyisocyanurate from the same lot as used herein yielded 18 resistivities and the following best fit (which is considered more accurate than the one in Figure 6):

$$r_{PIR} = 5.139 - 0.0101\ (T_{mean}\ (°F) - 75)\ \text{h·ft}^2\text{·°F/(Btu·in.)}$$
$$[= 35.63 - 0.1260\ (T_{mean}\ (°C) - 23.9)\ \text{m·K/W}].$$

The best fits for the glass wool and fiberboard are

$$r_{GW} = 3.591 - 0.0079\ (T_{mean}\ (°F) - 75)$$
$$[= 24.90 - 0.0981\ (T_{mean}\ (°C) - 23.9)]$$

and

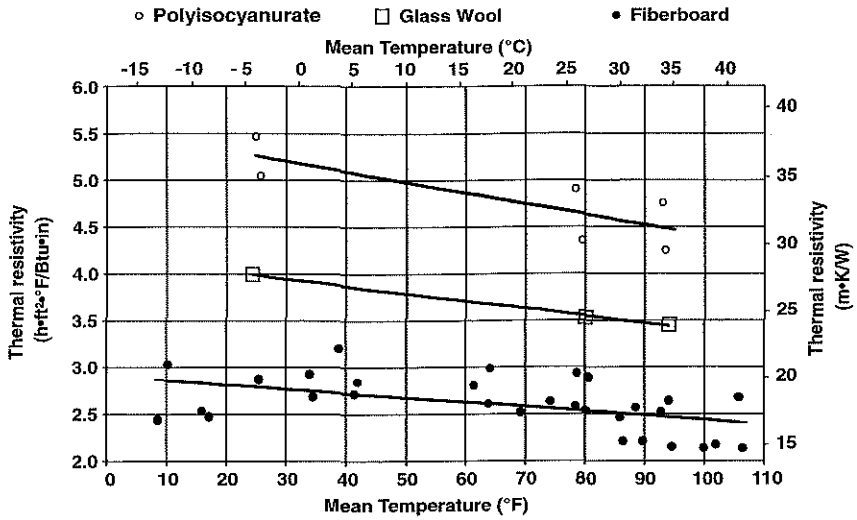

Figure 6 *In-situ measurements of the thermal resistivities of polyisocyanurate, glass wool, and fiberboard insulations in the test panels.*

$$r_{FB} = 2.560 - 0.0047\ (T_{mean}\ (°F) - 75)$$
$$[= 17.75 - 0.0589\ (T_{mean}\ (°C) - 23.9)],$$

respectively.

The total weights of the six test panels were monitored during the steady-state tests. They were constant during the first and second tests within ±0.02 lb (±9 g), which also happened to be the standard deviation of the average weight over all eight hours of these tests. For a normal distribution about the average of the 960 measurements (over eight hours at 30-second intervals), the 95% confidence interval would be twice the standard deviation or ±0.04 lb (±18 g). In the third steady-state test, the weights appeared to increase about 0.3 lb (0.14 kg) for all panels except Panel B. Its weight appeared to decrease about 0.2 lb (0.09 kg). The temperature of the air around the load cells was below freezing, and frost formed on some of the load cells during this test. Whether or not the panels gained or lost a small amount of water during the last steady-state test, they did contain moisture typical of construction dry materials at the beginning of the diurnal cycle tests.

Dynamic Dry Runs

Figure 7 shows the weight changes observed in the four diurnal cycle tests with construction dry panels. The total weight, written to the analysis spreadsheet for each test at five-minute intervals, was already the average of ten values scanned every 30 seconds and stored in the daily historical database. It was additionally averaged over 24 hours for each cycle. The first cycle of each test was used to allow the temper-

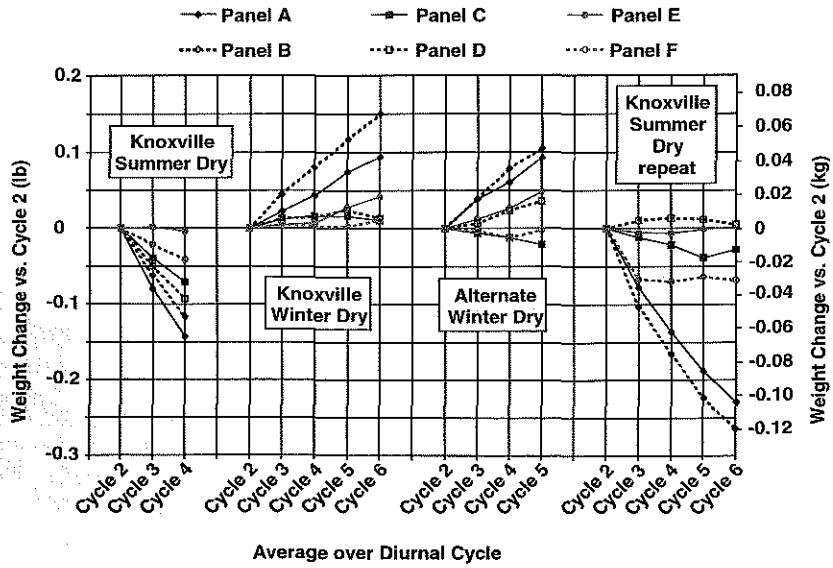

Figure 7 *Weight changes of the test panels in the construction dry diurnal cycle test.*

atures throughout the test panels to adjust to the imposed temperatures in the upper chamber. Weights are shown in Figure 7 as changes relative to the value for the second cycle of each test. They changed consistently from cycle to cycle for all panels and all tests within a random fluctuation of about ±0.02 lb (±9 g) and unexpected but consistent changes from −0.04 lb to +0.04 lb (−18 g to +18 g) for Panels E and F. This uncertainty of ±0.04 lb (±18 g) coincides with the limits of the 95% confidence interval estimated from behavior during the first two steady-state tests. The bottom membrane for the top-ventilated system of Panel E was intact for these runs, so it was identical in drying capability to the control system of Panel F. The reason for the large change in weight for Panel F for cycle 3 of the repeated Knoxville summer dry test is unknown. The weight of this panel behaves as expected for the rest of this test.

The first Knoxville summer dry test showed that all panels dried out more relative to their already construction dry configurations. From best fit straight lines through the data, the rates varied from −0.002 lb/day (1 g/day) for Panel F to −0.071 lb/day (−32 g/day) for Panel A. However, Panel B with the more permeable slotted deck did not dry quite as fast (−0.059 lb/day or −27 g/day) as Panel A with the less permeable solid deck. When this became apparent, this test was terminated and it was considered pre-conditioning for the subsequent diurnal tests. The dry tests are mainly to confirm that the thermal and hygric models of the configurations exhibit appropriate but small rates of weight gain or loss. Our experience has shown that this is a matter of adjusting the deck permeance in the models by trial and error.

In the winter dry and the repeated summer dry cycles, only Panels A and B exhibited significant changes in weight. This shows that these self-drying designs are indeed open to moisture exchange with the lower chamber. The slotted deck of Panel B allows slightly faster wetting and drying rates than the solid deck of Panel A, indicating that the deck permeance to water vapor is a significant variable for controlling rates of weight change. The effect of the slightly colder conditions in the alternate winter dry cycles is inconclusive. Panel A gained weight in the alternate winter cycles at +0.030 lb/day (+14 g/day) compared to +0.024 lb/day (+11 g/day) in the Knoxville winter cycles. However, Panel B gained at the same rate, +0.036 lb/day to 0.037 lb/day (+16 g/day to 17 g/day) in both. Notice in Figure 7 that the total weight gained by these panels in the winter cycles is lost during the repeated summer cycles before the end of the sixth cycle. As an indication that the self-drying designs are as dry as the vapor pressure in the lower chamber permits, the rates of loss for Panels A and B slow from −0.08 lb/day (−36 g/day) and −0.10 lb/day (−47 g/day), respectively, in the first repeat summer dry cycle, to −0.04 lb/day (−19 g/day) in the last repeat summer dry cycle for both.

Dynamic Wet Run

After the addition of liquid water to each test section and the resumption of the Knoxville summer cycles, the drying rates increased significantly for configurations that allowed drying due, most likely, to the higher vapor pressures in the panels. Figure 8 uses Panel A as an example of the detailed drying that took place in the repeated summer dry cycles and the summer wet cycles. The small symbols are hourly averages of the total weight of the example panel and are so close together, on the scale used for hours into the tests, that they appear to form a solid line. The diurnal nature of the temperature in the upper chamber shows through in the hourly averages. The panel loses weight rapidly during the daytime part of the cycles when temperatures are high in the upper chamber and moisture drive is downward. It regains some weight during the nighttime part of the cycles when temperatures fall

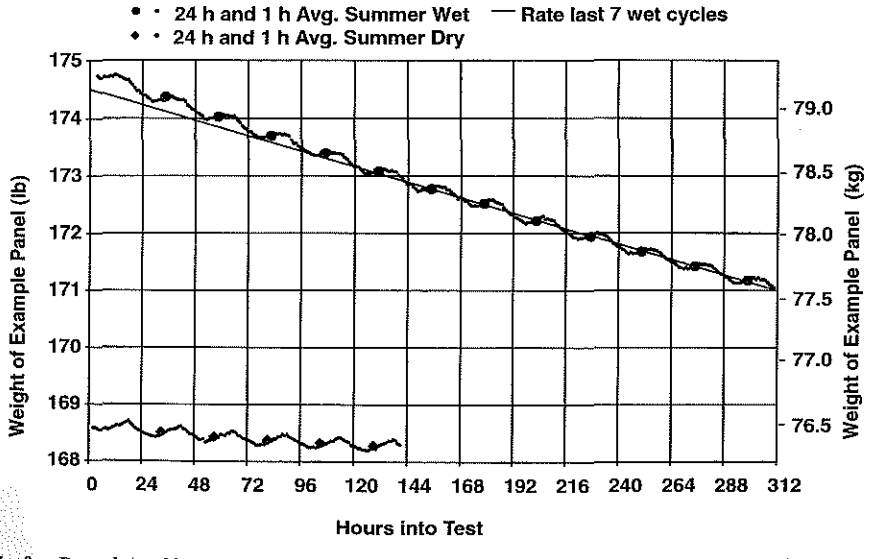

Figure 8 *Example for Panel A of hourly and daily average weight changes during summer dry and summer wet diurnal cycles.*

slightly below those in the lower chamber and moisture drive is upward. The net effect every 24 hours, shown by the large symbols, is a small rate of weight loss from the already construction dry panel. The water added to this panel (see Table 1) yielded a 6.5 lb (2.9 kg) weight gain from the end of the dry test to the beginning of the wet test. This amount was sufficient to yield a high but slightly decreasing weight loss rate in the first week of the test. This indicates too much water in the system for the quasi-steady daily average rates of weight change that would be consistent with the repeated identical temperature cycles imposed in the upper chamber, the constant temperature and relative humidity in the lower chamber, and movement of water throughout the panel at approximately constant rates until the amount is depleted to construction dry levels. The last week of the test yielded such quasi-steady daily average rates of drying, shown by the straight line through the large symbols.

Figure 9 shows, in the same way as Figure 7 did for the dry cycles, the weight change of each panel during the two additional weeks of Knoxville summer cycles after water was added. The 24-hour average drying rates during the last 5 to 7 cycles were steady. The scale of the weight changes in Figure 9 relative to Figure 7 reflects the abundance of water added to the panels, which Table 1 documented. All panels except Panels F and C show relatively large weight changes over the course of this test. In Panel F, the added water was trapped between impermeable polyethylene on the bottom and EPDM on the top. The liquid water permeable vapor retarders (WPVRs) in Panels C and D require the formation of condensate at the bottom of the system, which then can wick horizontally through the WPVRs and evaporate off their undersides. A possible explanation for the different behaviors of Panels C and D in Figure 9 is that the hygroscopic fiberboard in Panel C prevented condensate from forming while the permeable glass wool in Panel D did not. Liquid water properties for the WPVRs (Hansen 1986) indicate that 1.9 lb of water per 1 lb of WPVR (1.9 kg/kg) are required to initiate liquid moisture transfer through them, but only 1.0 lb/lb (1.0 kg/kg) is held at saturation. If any liquid water formed at the bottom of Panels C and D, it should have passed through the thin WPVRs.

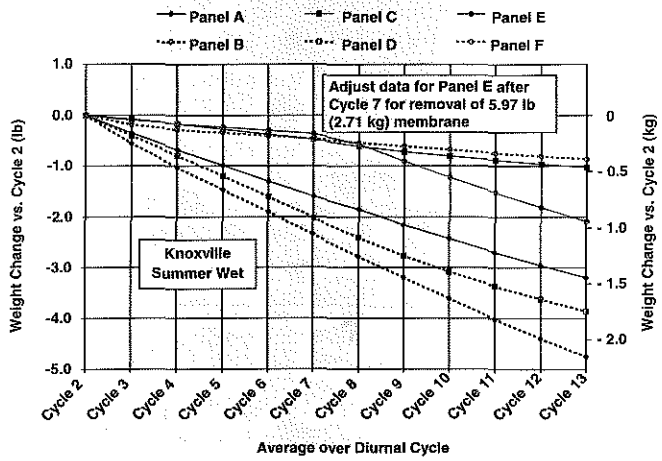

Figure 9 *Weight changes of the test panels in the diurnal cycle test after water addition.*

The top-ventilated system of Panel E depends upon wind action in actual applications to carry away water vapor that finds its way through the compromised lower membrane into the holes and slots in the EPS under the top membrane. There was no counterpart in the upper chamber to wind action except the flow of conditioned air in the chamber induced by circulation fans in the air-handler unit. Air speed was measured at approximately 3.6 mph (5.7 km/h) over the surface of Panel E. The lower membrane had only been compromised by cutting it with a utility knife in several places when the water was added. After cycle 7, it was removed entirely, and this appeared to allow the air circulation in the upper chamber to be effective.

Table 3 lists values for the rates of weight change for the diurnal cycles with the dry constructions and in the last week of the cycles after water was added. The data in Table 3 were calculated from the daily average rate of weight change for each panel, the same data used to prepare Figures 7 and 9, divided by the area of insulation, which was 19.8 ft^2 (1.84 m^2) in all panels. This form of the drying rates is chosen for direct comparison to the results of the thermal and hygric modeling.

TABLE 3

Rates of Weight Change per Unit Area of Insulation in Dry and Last Week of Wet Diurnal Cycles*

Panel	Knoxville Winter Dry	Alternate Winter Dry	Knoxville Summer Dry	Knoxville Summer Wet
A	+0.0012 (+5.9)	+0.0015 (+7.4)	−0.0039/−0.0021 (−19/−10)[a]	−0.014 (−67)
B	+0.0019 (+9.2)	+0.0018 (+8.8)	−0.0052/−0.0021 (−25/−10)[a]	−0.020 (−98)
C	+0.0001 (+0.6)	−0.0004 (−1.7)	−0.0004 (−2)	−0.005 (−24)
D	+0.0002 (+1.0)	+0.0006 (+3.1)	+0.00006 (+0.3)	−0.014 (−67)
E	+0.0005 (+2.6)	+0.0008 (+4.0)	+0.00005 (+0.3)	−0.015 (−75)[b]
F	+0.0001 (+0.5)	−0.00008 (−0.4)	+0.00001 (+0.05)	−0.003 (−16)

* Units are lb/day/ft^2 (g/day/m^2).
[a] Rates for first/last day of test.
[b] Rate after removal of membrane under top-ventilated system.

In the modeling, the same sunny summer or winter day temperature cycles shown in Figure 5 were repeated for 31 days, just like they were applied in the diurnal cycle tests for up to 14 days in the upper chamber. The drying rates that result from these repetitions of the same cycle day after day are likely different than actual summer or winter weather conditions would yield for the same total elapsed time but should be true on average. Further discussion of the measured rates is deferred until presentation of the modeling results.

MODELING RESULTS

The one-dimensional thermal and hygric model MATCH (Pedersen 1990) was applied to the self-drying designs (Panels A and B), the systems with liquid water-permeable vapor retarders (Panels C and D), and the impermeable control panel (Panel F). A model of the top-ventilated system (Panel E) was not attempted. For it, the drying, in which water vapor migrating into the holes in the EPS of the system for top-ventilation is picked up by the airflow in the slots, is not reasonably reduced to one-dimensional flow through a solid layer with specified permeance. Any airflow over the exposed flutes of the metal decks likely caused two-dimensional vapor flow out of the decks, too, but the solid and slotted decks were modeled as one-dimensional layers with vapor permeances of 17.5 perms and 87.5 perms [1.0×10^{-6} and 5.0×10^{-6} g/(s·m^2·Pa)], respectively. The values were established by trial and error over all runs. Thermal and hygric properties of the other materials in the systems were entered in a properties library used by MATCH. Polyisocyanurate, fiberboard, and glass wool properties were those of Burch and Desjarlais (1995). Properties for gypsum, the EPDM membrane, and the liquid water permeable vapor retarder were from Hansen (1986).

Table 4 summarizes the results of the modeling and compares the rates of weight change per unit area predicted by MATCH to the measured rates in Table 3 for the Knoxville winter dry and the Knoxville summer wet conditions. The low rates of weight gain measured during the winter dry tests are mirrored by the predictions although there is not as much difference between the predicted rates as there is between the measured rates for Panels A and B. This is despite the five times more permeable slotted deck. In the summer wet cycles, the same underprediction of the wetting rate occurs for Panel B relative to Panel A. To predict a larger rate for Panel B, even larger permeance for the slotted deck could be specified. This does not seem reasonable if the concept of permeance is applicable to the decks, which the model assumes. In the models for the summer wet situation, Panels C and D, with liquid water permeable vapor retarders, appeared to be nearly depleted of added water by the end of 31 days. Hence, rates are presented for the earlier time intervals given in the footnote.

TABLE 4
Rates of Weight Change per Unit Area of Insulation Predicted by Modeling vs. Measured Rates from Table 3*

	Knoxville Winter Dry		Knoxville Summer Wet	
Panel	**Measured**	**Predicted[a]**	**Measured**	**Predicted[b]**
A	+0.0012 (+5.9)	+0.0013 (+6.2)	−0.014 (−67)	−0.012 (−58)
B	+0.0019 (+9.2)	+0.0014 (+6.9)	−0.020 (−98)	−0.014 (−66)
C	+0.00013 (+0.6)	+0.00027 (+1.3)	−0.005 (−24)	−0.017 (−83)
D	+0.00020 (+1.0)	+0.00015 (+0.7)	−0.014 (−67)	−0.014 (−66)
F	+0.00010 (+0.5)	+0.00004 (+0.2)	−0.003 (−16)	−0.00008 (−0.4)

* Units are lb/day/ft² (g/day/m²)
[a] Rates for last 7 days of 31 days.
[b] Rates for last 6 days of 31 days except Panel C for days 17 through 24 and Panel D for days 21 through 27.

The large rate of weight loss measured for Panel F in the summer wet test relative to all the dry tests is somewhat disappointing. It is likely due to moisture escaping from the edges of the control panel. With so much water trapped between the impermeable vapor retarder and membrane of the control panel, it is not unreasonable that some escaped in this way. The drying rates for the other wet systems must be considered uncertain within the magnitude of the apparent drying rate of the control panel. Note that the predictions show a small rate of loss for Panel F in the summer wet cycles, with magnitude only twice that of the rate of gain in the winter dry cycles.

To provide more insight into the predictions and measurements, Figure 10 shows variations in the percentages of moisture by weight predicted for the components of Panels A and B, the self-drying designs, and Panels C and D, the systems with liquid water permeable vapor retarders. The models were run for 31 Knoxville summer days after water was added. The measurements only continued for 13 days. The layers of insulation shown in Figure 2 were further subdivided in the models for Panels A and B into two top layers of fiberboard (Top 1 FB and Top 2 FB) and two bottom layers of fiberboard (Bot 1 FB and Bot 2 FB), each 0.25 in. (0.64 cm) thick, between the 1 in. (2.5 cm) thick layer of polyisocyanurate (PIR) in each panel. In Panel C, the two 1 in. (2.5 cm) thick layers of fiberboard were modeled as a 1.5 in. (3.8 cm) thick layer (Mid FB) between two 0.25 in. (0.64 cm) thick layers (Top FB and Bot FB). The 4 in. (10.2 cm) thick piece of glass wool insulation in Panel D was divided in half in the model (Top GW and Bot GW). These subdivisions show more detail about the moisture movement. The total water content per unit area of each panel is also shown to aid comparisons.

With the solid deck under Panel A, the polyisocyanurate moisture content remains constant for all 31 days. The relatively impermeable deck causes slight moisture build up in the bottommost layers of fiberboard (Bot 1 FB and Bot 2 FB). With the slotted deck under Panel B, the moisture content is low in the polyisocyanurate and the bottommost layers of fiberboard. There is nothing relatively impermeable below them. Note that in Panels A and B, the moisture contents in the

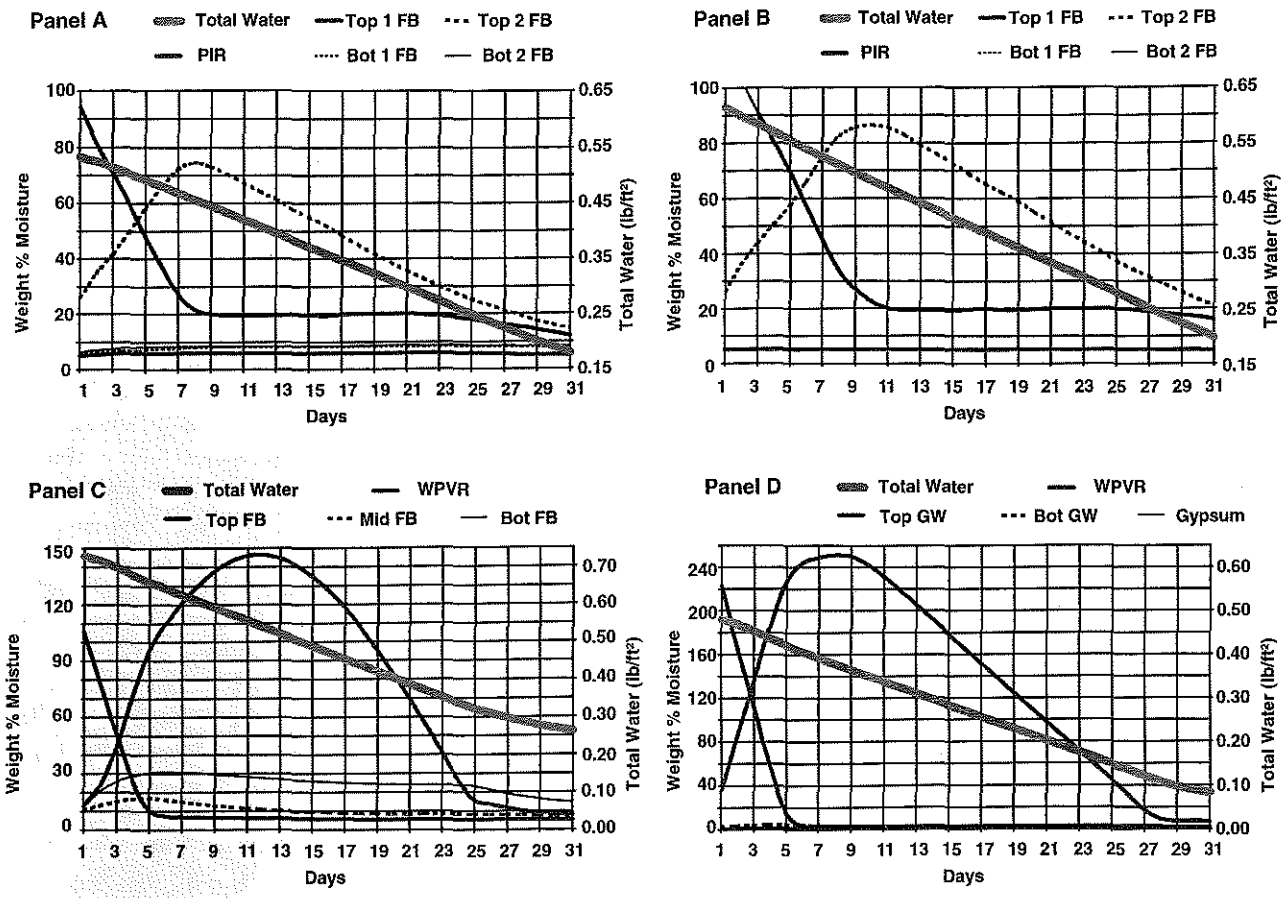

Figure 10 *Weight percent of moisture in the various layers of the models for Panels A through D during the Knoxville summer wet run.*

bottom half of the uppermost layer of fiberboard (Top 2 FB) is changing almost linearly after a week until near the end of the 31 days of modeling. Thus, the quasi-steady drying rate observed in the second week of the experiments is reasonable and should compare well to the predicted rates from the last six days of the 31 day model run. The models for both Panels A and B show a rapid decrease in the moisture content of Top 1 FB in the first eight days, which indicates that the excess water (>35% moisture content) was quickly driven downward. This layer stays safely at 20% moisture content for the next two weeks. There is a slight decrease in the moisture content of this layer in the last six days of the 31 days that the model was run. Other layers are not yet affected by the drying out of all the water that was added.

In both Panels C and D, the WPVR appears to control the rate of drying. Since it is not very thick but is more dense than the polyisocyanurate in Panels A and B, its weight percent moisture content is somewhat larger than that of the thicker but less dense polyisocyanurate. According to the model of Panel C, moisture is absorbed in the bottommost layer of fiberboard. In the experiment, this may have prevented the condensation needed on the WPVR for water to pass through it. Lack of condensation would inhibit the efficiency of the WPVR and yield a low rate of drying. The WPVR is also not as impermeable to water vapor as solid polyethylene. The lower vapor pressure in the bottom of Panel C from absorption of water in the fiberboard could also lower the rate of drying.

The model of Panel C showed a steady rate of drying from 13 to 24 days. As reported in Table 4, the rate is larger than that for Panel D from 11 to 27 days. In the experiments with Panel D, the WPVR seems to have functioned as designed and the predicted rate agrees exactly with the measured rate in the last six days of the test. The models for both Panels C and D predict that drying is essentially complete by the end of 31 days of average sunny Knoxville summer cycles. They also show that moisture content in the WPVRs was not very linear from 7 to 14 days, especially for Panel C. The 13 days of the summer test after water was added were barely enough to achieve the quasi-steady conditions needed for measuring a drying rate comparable to the steady value reported for the model. However, like Panels A and B, Panels C and D seemed to have excess (>35% moisture content for fiberboard) water added, which quickly flowed downward in the systems.

The detailed component moisture contents for the Knoxville winter dry run showed that all components gained moisture linearly throughout the 31 days of modeling, except for a

few days at the beginning. This supports the good agreement between measurements and predictions in Table 4 for the winter dry conditions. By the end of the 31 days at winter conditions, the top fiberboard's moisture content in Panels A and B was still under 30% by weight, safely below the 35% saturation level.

MATCH was also run for the Knoxville summer dry condition after the winter dry runs. Moisture contents in Panels A and B were changing throughout the first seven days. This supports the differing rates that are reported in Table 2 for the first and last days of this six-cycle experiment. By the end of the 31 days that the model was run, drying rates were an order of magnitude smaller than the values given in Table 3 for the last day (day 7) of the repeat summer dry test. To start the models for the summer wet simulations, moisture contents in the panels were adjusted to reflect the actual amount of water in each panel. The extra drying from the longer run of the model at summer dry conditions did not affect the comparisons above the between measurements and predictions for the summer wet condition.

CONCLUSIONS

Simultaneous experiments on the moisture behavior of various low-slope roof systems have been performed in a large-scale climate simulator. Total weight of each test panel was measured and recorded continuously, along with temperatures and heat fluxes, to compare the behavior of the various systems before and after water was deliberately added to all, and all experienced the same conditions. The systems comprised a self-drying design over a conventional metal deck, a self-drying design over a significantly more permeable slotted metal deck, and four others over conventional metal decks: a system typical of U.S. construction with a liquid water permeable vapor retarder, a system typical of European construction with a liquid water permeable vapor retarder, a top-ventilated system with a polyethylene vapor retarder, and an impermeable control system with a polyethylene vapor retarder. All systems except the top-ventilated system were modeled before and after water was added with the one-dimensional thermal and hygric model MATCH. This work has shown the following:

- The suspension of typical constructions from load cells for a record of total weight and the modeling with MATCH for information per unit area is a good combination for obtaining detailed information on the relative moisture performance of different low-slope roof constructions. Better model verification would be obtained if we could unobtrusively measure the moisture content as a function of time at various places within the construction.
- The self-drying roof design as tested at Knoxville summer conditions after water was added, in combination with a permeable deck, dried more rapidly than the European water permeable vapor retarder and top-ventilated systems, even after the bottom membrane was removed entirely from the top-ventilated system. With the same less permeable deck as the European water permeable vapor retarder system, its drying rate is about the same as the European system and the uninhibited top-ventilated system.
- The self-drying roofs, which had no vapor retarders at all, wetted faster at winter conditions than the systems with liquid water permeable but water vapor impermeable vapor retarders. However, maximum fiberboard moisture content remained safely below saturation levels in all systems after a month of average winter sunny days.
- At summer conditions after water is added, placement of a hygroscopic material like fiberboard on top of the liquid water permeable vapor retarder appears to inhibit performance of the system, as evidenced by the low drying rates measured for the U.S. liquid water permeable vapor retarder system relative to the European version and the self-drying roof designs. The thermal and hygric model of the water permeable vapor retarder allowed the U.S. version to dry faster than the European system at the conditions that were modeled, suggesting the need for a better hygric model of the liquid water permeable vapor retarder system to match test conditions regarding condensation.
- Models of the self-drying roofs and the liquid water permeable vapor retarder systems both show that a month of drying with average sunny Knoxville summer days is enough to dry out the average 8.0 lb (2.9 kg) of water added to the 19.8 ft^2 (1.84 m^2) cross-sectional area and varying insulation thickness and density in these panels. The two weeks of experiments at summer conditions conducted after water was added were not enough to measure this much drying. The cost and the difficulty of keeping a large-scale climate simulator and all the instrumentation in continuous operation for times longer than a few weeks make models the only practical way to get monthly and yearly information under controlled conditions. A few weeks of experiments are sufficient to calibrate the models.
- The water added certainly represented an appreciable leak into a roofing system since it increased the moisture content of the top layers of fiberboard in the systems well above 35%. It is interesting to note that the bottom layer of fiberboard in the self-drying roof designs and the U.S. construction with a liquid water permeable vapor retarder did not ever reach saturation. Therefore, if there were no pathways for water leakage through cracks in joints between pieces of construction materials inside the roof, leakage into the building interior would not be a problem for this combination of leakage, roof type, and climate.

REFERENCES

ASTM. 1989. ASTM C 236-89, Standard test method for steady-state thermal performance of building assemblies by means of a guarded hot box. *Annual Book of Standards*, Vol. 04.06, pp. 53-63. Philadelphia, Pa.: American Society for Testing and Materials.

ASTM. 1992. ASTM C 518-91, Standard test method for steady-state heat flux measurements and thermal transmission properties by means of the heat flow meter apparatus. *Annual Book of Standards*, Vol. 04.06, pp. 153-164. Philadelphia, Pa.: American Society for Testing and Materials.

Burch, D.M., and A.O. Desjarlais. 1995. Water-vapor measurements of low-slope roofing materials. Report NISTIR 5681. Gaithersburg, Md.: National Institute of Standards and Technology.

Desjarlais, A.O., J.E. Christian, D.M. Kyle, and C. Rode (formerly C.R. Pedersen). 1993. Moisture: Its effects on the thermal performance of a low-slope roof system. *ASHRAE Transactions* 99(2).

Desjarlais, A.O., D.M. Kyle, P.W. Childs, and J.E. Christian. 1994. Laboratory measurements of the drying rates of low-slope roofing systems. *Proceedings of the Low-Slope Reroofing Workshop*, pp. 77-88. Report No. CONF-9405206. Oak Ridge, Tenn.: Oak Ridge National Laboratory.

Hansen, K.K. 1986. Sorption isotherms. A catalogue. Technical Report TR 162/86. Lyngby, Denmark: Technical University of Denmark.

Kyle, D.M., and A.O. Desjarlais. 1994. Assessment of technologies for constructing self-drying low-slope roofs. Report ORNL/CON-380. Oak Ridge, Tenn.: Oak Ridge National Laboratory.

Motakef, S., and L.R. Glicksman. 1989. A capacitance probe for measurement of moisture content in open pore thermal insulations. Report No. ORNL/Sub/85-27486-1. Oak Ridge, Tenn.: Oak Ridge National Laboratory.

NRCA. 1996. Some of the design considerations and references for design information regarding self-drying roofs. *NRCA Roofing and Waterproofing Manual—Fourth Edition, Volume 1*. Low-Slope Roofing Text, Section 7.2.3. Rosemont, Ill.: National Roofing Contractors Association.

Pedersen, C.R. 1990. Combined heat and mass transfer in building constructions. Ph.D. Thesis, Technical University of Denmark, Thermal Insulation Laboratory.

Pedersen, C.R., T.W. Petrie, G.E. Courville, A.O. Desjarlais, P.W. Childs, and K.E. Wilkes. 1992. Moisture effects in low-slope roofs: Drying rates after water addition with various vapor retarders. Report No. ORNL/CON-308. Oak Ridge, Tenn.: Oak Ridge National Laboratory.

Powell, F.J., and H.E. Robinson. 1971. The effect of moisture on the heat transfer performance of insulated flat-roof constructions. Building Science Series Report 37. Gaithersburg, Md.: U.S. National Bureau of Standards.